Revista Ciência Agronômica, v. 53, e20207797, 2022
Centro de Ciências Agrárias - Universidade Federal do Ceará, Fortaleza, CE
www.ccarevista.ufc.br

Scientific Article
ISSN 1806-6690

The use of computer vision to classify Xaraés grass according to nutritional status in nitrogen[1]

Uso de visão computacional na classificação de capim Xaraés segundo o status nutricional em nitrogênio

Wellington Renato Mancin[2], Lilian Elgalise Techio Pereira[3], Rachel Santos Bueno Carvalho[2], Yeyin Shi[4], Wilson Manuel Castro Silupu[5], Adriano Rogério Bruno Tech[2]*

ABSTRACT - This study is based on the principle that vegetation indexes (VIs), derived from the RGB color model obtained from digital images, can be used to characterize spectral signatures and classify *Brachiaria brizantha* cv. Xaraés according to nitrogen status (N). From colorimetric data obtained from leaf blade images acquired in the field, three artificial neural networks were evaluated according to the performance in the classification of N status: Feedforward Backpropagation (FFBP), Cascade Forward Backpropagation (CFBP) and Radial Base function (RBFNN). Four N fertilization rates were applied to generate contrasting N contents in the plants. The youngest completely expanded leaves from 60 tillers were detached at each regrowth cycle of 28 days, thus their images and leaf N content were obtained. Samples were then classified as deficient (< 17 g N kg^{-1} leaf dry matter (DM), moderately deficient (from 17.1 to 20.0 g N kg^{-1} DM), and sufficient (> 20.1 g N kg^{-1} DM). The VIs were selected by principal component analysis and the performance of the networks evaluated by the accuracy. The accuracy in classification obtained by the networks were 88%, 86% and 79% for FFBP, CFBP and RBFNN, respectively, indicating that the spectral signatures can be determined from images acquired in the field. So, the proposed method could be used to develop a software that aims to monitor the status of N in real time, providing a fast and inexpensive tool for defining the time and the amount of N fertilizer, according to the pasture demand.

Key words: Image processing. Remote sensing. HSB. Spectral signature.

RESUMO - Este estudo baseia-se no princípio de que índices de vegetação (IVs), derivados do modelo de cores RGB obtidos de imagens digitais, podem ser usados para caracterizar assinaturas espectrais e classificar pastos de *Brachiaria brizantha* cv. Xaraés segundo o status de nitrogênio (N). A partir de dados colorimétricos obtidos de imagens de lâminas foliares adquiridas em campo, três redes neurais artificiais foram avaliadas quanto ao desempenho na classificação do status N: Feedforward Backpropagation (FFBP), Cascade Forward Backpropagation (CFBP) e função de Base Radial (RBFNN). Quatro taxas de fertilização nitrogenada foram aplicadas para gerar contrastes no teor de N nos tecidos das plantas. As folhas mais jovens completamente expandidas de 60 perfilhos foram destacadas das plantas a cada ciclo de rebrotação de 28 dias, sendo as imagens das folhas e teor de N foliar determinados. As amostras foram classificadas em deficientes (< 17 g N kg^{-1} de matéria seca (MS)), moderadamente deficientes (de 17,1 a 20,0 g N kg^{-1} MS) e suficiente (> 20,1 g N kg^{-1} MS). Os IVs foram selecionados pela análise de componentes principais e o desempenho das redes avaliados pela acurácia. As acurácias nas classificações obtidas pelas redes foram de 88%, 86% e 79% para FFBP, CFBP e RBFNN, respectivamente, indicando que as assinaturas espectrais podem ser determinadas a partir de imagens adquiridas em campo. Assim, o método proposto pode ser utilizado para desenvolver um software de monitoramento do status de N em tempo real, fornecendo uma ferramenta rápida e econômica para definir o momento e quantidade de fertilizantes nitrogenados, conforme demanda da pastagem.

Palavras-chave: Processamento de imagens. Sensoriamento remoto. HSB. Assinatura espectral.

DOI: 10.5935/1806-6690.20220006
Editor-in-Article: Profa. Andrea Pereira Pinto - deiapp@hotmail.com
*Author for correspondence
Received for publication on 17/12/2020; approved on 12/07/2021
[1]Parte da Dissertação do primeiro autor, apresentada ao Programa de Pós-Graduação em Gestão e Inovação na Indústria Animal da Faculdade de Zootecnia e Engenharia de Alimentos (FZEA/USP)
[2]Departamento de Ciências Básicas (ZAB), Faculdade de Zootecnia e Engenharia de Alimentos (FZEA/USP), Pirassununga-SP, Brasil, wellmancin@gmail.com (ORCID ID 0000-0002-4242-1327), adriano.tech@usp.br (ORCID ID 0000-0003-2628-1915), rbueno@usp.br (ORCID ID 0000-0002-0555-1480)
[3]Departamento de Zootecnia (ZAZ), Faculdade de Zootecnia e Engenharia de Alimentos (FZEA/USP), Pirassununga-SP, Brasil, ltechio@usp.br (ORCID ID 0000-0002-3022-8423)
[4]Department of Biological Systems Engineering, University of Nebraska-Lincoln, Lincoln, NE 68583, USA, yshi18@unl.edu (ORCID ID 0000-0003-3964-2855)
[5]Facultad de Ingeniería de Industrias Alimentarias, Universidad Nacional de Frontera, Sullana 20103, Peru, wcastro@unf.edu.pe (ORCID ID 0000-0001-7286-1262)

INTRODUCTION

Brazil has the largest cattle herd in the world, with approximately 90% of it raised and finished on pastures. However, livestock production has been considered a major contributor to greenhouse gas (GHG) emissions (MAZZETTO *et al.*, 2015). Despite the productivity gains observed in recent decades, the challenges for Brazilian pasture systems still remain, mainly by low productivity and soil fertility, due to the lack of nutrient replacement and degradation of pastures (SANTOS; PRIMAVESI; BERNARDI, 2010; SILVA *et al.*, 2017). In this context, while for some countries reducing the annual amount of fertilizer applied on pastures may play a significant role in the mitigation effort thereof, in Brazil, the intensification of pasture-based livestock production is thought to lead to higher animal performance, reduced time until slaughter, better soil fertility and increased soil carbon stocks, thus reducing the pasture area and GHG emissions per kg of product (CARDOSO *et al.*, 2016).

Nitrogen is well known to be essential for pasture growth and productivity by its stimulus to the tillering, leaf growth and photosynthetic processes (YASUOKA *et al.*, 2018). Thus, real-time identification of the N status is essential for increasing the efficiency and ensuring environmental quality, once insufficient N supply leads to lower chlorophyll content, less biomass production and poor soil covering; and their excessive application can lead to soil, water and environment pollution (CARDOSO *et al.*, 2016; GAUTAM; PANIGRAHI, 2007; WANG *et al.*, 2014).

Remote sensing techniques have emerged as important tools for monitoring crop growth, plant stress and its nutritional status, and most of those techniques have been based on image analysis. Those application rely on the principle that relationship among the spectral reflectance of the leaves or canopy may be correlated with canopy growth traits, plant nutrients status and productivity, and the relationships can be described by exploring information contained in images (WANG *et al.*, 2014). Many research efforts have been dedicated to the image processing software development capable of determining the plant nutrient status through images acquired by scanners, commercial digital cameras, or even by cellphone and smartphone cameras, generating information to support decision making on fertilization strategies (BARESEL *et al.*, 2017; HU *et al.*, 2013; LEE; LEE, 2013; MOHAN; GUPTA, 2019; ZILBERMAN *et al.*, 2018).

Taking into account that N is one of the main structural components of chlorophyll, and that changes in the N content of the plant are visually expressed by alterations in the color, the leaf color has been recognized as one of the most sensitive indicator of the plant N status (TEWARI *et al.*, 2013). However, successful prediction of plant nutritional status is largely dependent upon the identification of wavelength reflectance (spectral signatures) or any color index (vegetation indices, VIs), that strongly correlate with the plant N content.

The selection of key IV's aiming at to define the plant's N status or their N content has been greatly improved by the use of multivariate statistical methods (Yi *et al.*, 2007), such as principal component analysis (PCA), integrated to the processing, identification of patterns and classification by using artificial neural network (ANN) models. The ANN models have been widely used as tools for dynamic modeling (SHARABIANI; NAZARLOO; TAGHINEZHAD, 2019) in the programming of the computer vision systems, being capable of associating several image spectral information with target attributes (crop attribute) (HE *et al.*, 2011; SAFA *et al.*, 2019).

Based on this background, the main goal was to test the prediction of N status from images of leaves of *Brachiaria brizantha* 'Xaraes' using the red, green and blue components and their derivative indices (vegetation indices) applied the artificial neural networks.

MATERIAL AND METHODS

Experimental field treatments

The experiment was carried out at the Faculty of Animal Science and Food Engineering (FZEA), University of São Paulo, Pirassununga (21°57'31'' S, 47°27'07' W, 620 m a.s.l.), SP, Brazil. In the experimental area, the slope is moderately undulating and the soil is classified as Typic Eutrudox (USDA Soil Taxonomy) or dystrophic Red Latosol (EMPRESA BRASILEIRA DE PESQUISA AGROPECUÁRIA, 2018). Climate in the region is Cwa, sub-tropical with dry winter, and the annual average rainfall is 1,343 mm (EMPRESA BRASILEIRA DE PESQUISA AGROPECUÁRIA, 2019). The monthly average temperature during the experimental period (December 2017 to March 2018) was 23.7°C and the monthly rainfall corresponded to 151.6, 82.0, 209.8 and 148.2 mm during the successive evaluation cycles.

The vegetal species *Brachiaria brizantha* 'Xaraes' was established in 2012, and the experimental area comprised of 12 plots of 20 m^2 (5 m x 4 m) each. Due to possible differences in the initial soil fertility, the experimental area was organized in blocks, from which soil samples were collected at 0-20 cm soil depth in October 2017. Average soil chemical characteristics for the 0–20 cm layer were: pH $CaCl_2$ = 4.5, 5.2 and 4.9; organic matter = 21.4, 24.4 and 24.1 g kg^{-1}; P (resin) = 12.0, 13.0 and 10.0 mg.dm^{-3}; Ca = 9.0, 21.0 and 15.0 mmolc.dm^{-3}; Mg = 3.0, 6.0 and 3.0 mmolc.dm^{-3}; K =

2.2, 2.4 and 2.8 mmolc.dm^{-3}; H + Al = 33.4, 26.8 and 26.5 mmolc.dm^{-3}; soil base saturation = 30, 52 and 44%, respectively for blocks 1, 2 and 3 and composed by 64 g kg^{-1} clay, 46 g kg^{-1} silt and 31 g kg^{-1} sand . The results were used to determine the requirements of fertilization aiming at soil nutrients correction.

For homogenization of the experimental plots and preparation for the beginning of the experiment, mowing was carried out in October 20, 2017. Afterwards, the plants were cut every 28 days, using a manual mower, leaving a residual height of 15 cm (PEDREIRA; PEDREIRA; SILVA, 2007). During the first regrowth cycle (October 20 to November 15, 2017), soil nutrients correction was performed in each plot by using the amount of 45 kg P_2O_5 ha^{-1} (Triple superphosphate, 43% P_2O_5) and 30 kg K_2O ha^{-1} (Potassium chloride, 60% K_2O). The remaining phosphorus and potassium fertilizers were applied in December 01, 2017, by using the amount of 15 kg P_2O_5 ha^{-1} and 10 kg K_2O ha^{-1}.

The experimental evaluations were carried out from the second harvest onwards and, thus, the monitored cycles corresponded to the periods: (1) from November 15 to December 13, 2017; (2) December 13, 2017 to January 10, 2018; (3) January 10 to February 9, 2018 and (4) February 9 to March 10, 2018. Field treatments consisted of four nitrogen fertilization rates, defined in order to generate contrasting N content in the plants, as follows: no nitrogen (N0), 15 (N15), 30 (N30) and 45 (N45) kg of N ha^{-1} per cutting by using ammonium nitrate (32% N), and fertilizers were applied after each cutting. The experiment used a completely randomized block design, with three replications, and the blocking criterion was the initial soil fertility.

Leaf sampling, image acquisition and N content determination

The youngest completely expanded leaves (diagnostic leaf) from 60 tillers randomly chosen into the plots were detached from plants. Five samples composed of five leaves, which were placed side by side on an image-collecting table, were used during the image acquisition procedure. The image-collecting table was built using a black matte background, with a fixed support for the cellphone camera to acquire images, positioned at a fixed height of 23 cm from the base. Five images per plot from different groups of leaves were acquired from 08:00 to 11:00 a.m. on sunny days at each regrowth cycle. In order to mimetize the possibilities of field capturing, images were acquired in shade, but without other procedures of environment lighting standardization. A 16-megapixel back camera of a Lenovo-Motorola K6 Plus cellphone set to automatic focus adjustment and flash off was used for images acquisition. Thus, the dataset of digital images was composed by 240 images (12 plots x 5 images x 4 regrowth cycles). However, ten images were removed from the dataset due to incongruencies in the images acquisition (overlapping of leaves), which affected their associated R, G and B values.

The digital images were stored in JPEG format (24 bits color) with resolution of 800 x 600 pixels. After image acquisition, the leaves from each plot were grouped (composed sample), then put into an oven to dry at 65 ºC until constant weight, and subsequently ground using a 1 mm sieve. Nitrogen content was determined by the Kjeldahl method after acid digestion (NOGUEIRA *et al.*, 1998), and the results were expressed in g N kg^{-1} leaf dry weight (DW). A total of 48 leaves samples was included in the dataset of N content, and for each sample there were 5 associated images.

The critical N content for a given crop represents its minimum N in the leaves essential to attain at least 80% of the maximum crop growth rate, and it is represented by a negative power function called “dilution curve” (ATA-UL-KARIM *et al.*, 2017). Costa *et al.* (2015) found that the critical N content of xaraes palisadegrass varied from 18.0 to 19.4 g N kg^{-1} DW, respectively to the dry and rainy seasons, when testing a range of N fertilization rates from 50 to 400 kg N ha^{-1}. Based on these values, and for the purpose of the present experiment, it was defined that the plants showing an N content below 17 g N kg^{-1} DW were deficient. Plants showing a range from 17.1 to 20.0 g N kg^{-1} DW were considered moderately deficient, while plants above 20.1 g N kg^{-1} DW were considered as having a sufficient N content.

Image processing and vegetation indices (VIs) determination

First, the images were pretreated by applying a low-pass filter (median filter), in order to remove noise (ZHU; HUANG, 2012). This nonlinear filter increases impulse noise ability while maintaining good edge keeping characteristics, eliminating lines and other fine details that do not belong to the image.

Next, the image was converted to grayscale (h) and the regions of interest (ROI), pixels with leaves information, were obtained by thresholding method (Otsu), Eq. (1).

$$I_{(x,y)} = \begin{cases} 1 \; if \; h_{(x,y)} \geq T \\ 0 \; if \; h_{(x,y)} < T \end{cases} \quad (1)$$

where: h is the image in grayscale; I, segmented image, (x, y), pixel position and T, thresholding value obtained by using Otsu method.

By applying a scanning algorithm (pixel to pixel), ROI was converted to the corresponding color of the

leaves by taking the original RGB values of each pixel, and the background was converted to white. The processed image was then subjected to a pixel-by-pixel analysis, from which the average values of R, G and B of the entire image were acquired, and from these values fifteen other color indices were calculated (or vegetation indices, Table 1), being the generated image saved in JPEG file. All the functions, scripts and user interfaces were implemented in Java language, using the NetBeans platform, version 8.2.

Principal component analysis (PCA)

A principal component analysis (PCA) was carried out in order to remove the lower-level components without any notable loss of information contained in the original dataset (YI *et al.*, 2007) using the Minitab® Software (version 2018). The dataset included in the PCA analysis consisted of 18 input variables: R, G and B intensities extracted from the images and their normalized values (R_N, G_N and B_N) as well as the hue (H), saturation (S) and brightness (Br) parameters, besides the vegetation indices VARIgreen, ExG, ExR, MExG, ExGR, CIVE, VEG, COM and DGCI (Table 1). The input variables were standardized to a mean of 0 and variance of 1, and significant variables were considered when eigenvectors were higher than 0.28. After the exploratory analysis, 12 indexes were selected for the dataset of the neural networks.

Artificial Neuronal Network (ANN) implementation

Based on ANN technique three different models were built using the MATLAB® (Matrix Laboratory) software, version 2015a. The ANN tested were radial basis function (RBFNN), multilayer feedforward backpropagation (FFBP), cascade forward backpropagation (CFBP). For FFBP and CFBP, the topology was tested using only one hidden layer and 5, 10 or 15 neurons, which were empirically chosen, and the learning algorithm Levenberg-Marquardt (LM) was used for such ANN models. The input dataset was composed by the 12 vegetation indexes selected by PCA and the nitrogen fertilization rates. Combinations among two transfer functions were also tested, TANSIG and LOGSIG (YI *et al.*, 2007, 2010), aiming at identifying the enhanced network arrangement. However, the LOGSIG function showed poor performance and was removed from the test procedures. The learning rate used in the training was 0.1 and the number of iterations was 1.500.

The performance of the ANN models was evaluated through the coefficient of determination (R^2) (Eq. 2) and Accuracy (Eq. 3). For network training, 70% of the data were used, the remaining 30% was used for network validation (15%) and performance testing (15%), and observations for validation and test were randomly selected. To test the RBFNN, the initial center value determined from

Table 1 - Vegetation indices (VIs) based on the RGB color space extracted from images, used to determine the N status in *Brachiaria brizantha* 'Xaraes'

[1]VIs	Formulae	References
G_N	$G_N = G/(R+G+B)$	Yang *et al*., (2015)
R_N	$R_N = R/(R+G+B)$	Yang *et al*., (2015)
B_N	$B_N = B/(R+G+B)$	Yang *et al*., (2015)
H	H= 60*{(G-B)/[max(R,G,B)-min(R,G,B)]}, if max(R,G,B)=R; or 60*{2+{(B-R)/[max(R,G,B)-min(R,G,B)]}}, if max(R,G,B)=G; or 60*{4+{(R-G)/[max(R,G,B)-min(R,G,B)]}}, if max(R,G,B)=B	Wang *et al*., (2014)
S	S = (max(R,G,B)-min(R,G,B))/max(R,G,B)	Wang *et al*., (2014)
Br	Br = max(R,G,B)/255	Wang *et al*., (2014)
VARIgreen	VARIgreen = (G-R)/(G+R-B)	Gitelson *et al*., (2002)
DGCI	DGCI = [(Hue − 60)/60 + (1 − Saturation) + (1 − Brightness)]/3	Karcher and Richardson (2003)
ExG	$ExG = (2*G_N)-R_N-B_N$	Guijarro *et al*., (2011) and Yang *et al*., (2015)
ExR	$ExR = (1.4*R_N)-G_N$	Guijarro *et al*., (2011)
ExGR	ExGR = ExG – ExR	Guijarro *et al*., (2011) and Yang *et al*., (2015)
MExG	MExG = 1.262*G - 0.884*R - 0.311*B	Burgos-Artizzu *et al*., (2011)
CIVE	$CIVE = 0.441R_N - 0.811G_N + 0.385B_N + 18.78745$	Guijarro *et al*., (2011) and Yang *et al*., (2015)
VEG	$VEG= G_N/(R_N^{0.667})*(B_N^{0.333})$	Guijarro *et al*., (2011) and Yang *et al*., (2015)
COM	COM = 0.25ExG + 0.30ExGR + 0.33CIVE + 0.12VEG	Yang *et al*., (2015)

[1] G_N, R_N and B_N represent normalized Green, Red and Blue, respectively; H, S and Br represent hue, saturation and brightness, respectively; VARIgreen represents the Visible Atmospherically Resistant Index; DGCI represents the Dark Green Color Index; ExG, ExR and ExGR represent excess of green, excess of red and excess of green minus excess of red; MExG is the modified excess of green; CIVE represents Colour Index of Vegetation Extraction; VEG represents the Vegetative Index and COM a Combined Index

the input data taken randomly was initiated using the K-means algorithm, the Euclidean distance norm was defined to measure the distance between input vector P and node j of the hidden layer, in which the spread value was 1 and the goal was 0.0001, and a Gaussian function transferred Euclidean distance to give output to each node (RAHMAT; NABABAN, 2018).

$$R^2 = \frac{SQ\,\mathrm{Re}\,g}{SQTotal} \quad (2)$$

where: R^2 is the coefficient of determination; SQReg is the variation in Y explained by the adjusted regression; SQTotal is the total variation in Y.

$$Accuracy = \frac{(TP + TN)}{(TP + TN + FP + FN)} \quad (3)$$

where: TP is true positive; TN is true negative; FP is false positive; FN is false negative.

RESULTS AND DISCUSSION

Images spectral signature of xaraes palisadegrass in response to leaf N content

Traditional procedures to monitor the N content based on laboratory analysis are time consuming, but they have been widely replaced by other faster and cheaper tools, such as the leaf color charts (INTARAVANNE; SUMRIDDETCHKAJORN, 2015) and/or portable chlorophyll meters (SCHLICHTING *et al*., 2015). Additionally, more recently, a wide range of remote proximal sensing technologies have been successfully employed (VERGARA-DÍAZ *et al.*, 2016) for estimation and monitoring the N status in various crops.

For these purposes, the identification of the spectral signature of the vegetation provides key parameters for detection of the plant nutritional status (SRIDEVY *et al.*, 2018). However, the evaluation of spectral signature requires spectrometric equipment and multispectral sensors, according the wavelengths of interest, which are normally costly. According to Vesali *et al.* (2015), the recent development of smartphones has opened new opportunities for high quality image capturing and data generation, making possible to use them for color analysis, with potential to substitute both spectral indices and chlorophyll measurements since information from the basic colors of red, green and blue (RGB) can describe the leaf spectral signature with similar accuracy.

In a general way, plants adequately supplied with N are greener because chlorophyll is a poor absorber of green and near-infrared (NIR) portions of the spectrum, and then the green light band (around 550 nm) is reflected more efficiently. In addition, the higher the photoactive pigments and chlorophyll content, the higher the absorption at blue and red wavelengths (ZILBERMAN *et al.*, 2018). The blue component has been less variable across gradients of leaf N or leaf pigments content in several species (EL-AZAZY, 2018; HU *et al.*, 2013). In the present experiment, the R and G components varied, respectively, from 151.1 ± 1.03 and 176.4 ± 1.04 in images representing deficient plants (< 17.0 g N kg^{-1} leaf DW) to 140.9 ± 0.83 and 164.4 ± 0.78 in images representing plants with sufficient N (> 20.1 g N kg^{-1} leaf DW). However, there was a slight increase in the values of the blue component from 109.1 ± 1.06 to 118.4 ± 1.44 for the respective classes (Table 2 and Figure 1a).

Table 2 - Variations of vegetation indices (VIs) according to the deficient, moderately deficient, sufficient classes, p-values and coefficient of determination for quadratic models (R^2)

VIs of images	Sufficient plants	Moderately deficient plants	Deficient plants	p-value Quadratic model	R^2 Quadratic model
R	140.9 ± 0.83	143.9 ± 0.85	151.1 ± 1.03	< 0.0001	0.26
G	164.4 ± 0.78	167.2 ± 0.90	176.4 ± 1.04	< 0.0001	0.31
B	118.4 ± 1.44	118.1 ± 1.22	109.1 ± 1.06	< 0.0001	0.12
R_N	0.33 ± 0.0008	0.33 ± 0.0005	0.34 ± 0.0007	< 0.0001	0.47
G_N	0.39 ± 0.001	0.39 ± 0.001	0.40 ± 0.0009	< 0.0001	0.26
B_N	0.28 ± 0.002	0.27 ± 0.002	0.25 ± 0.001	< 0.0001	0.39
H	91.9 ± 0.62	88.8 ± 0.46	82.9 ± 0.39	< 0.0001	0.47
S	0.28 ± 0.008	0.29 ± 0.007	0.38 ± 0.005	< 0.0001	0.34
Br	0.64 ± 0.003	0.66 ± 0.004	0.69 ± 0.004	< 0.0001	0.31
[1]ExG	0.16 ± 0.005	0.17 ± 0.004	0.21 ± 0.003	< 0.0001	0.24
ExR	0.077 ± 0.001	0.079 ± 0.001	0.080 ± 0.001	= 0.0293	0.031
CIVE	18.7 ± 0.002	18.7 ± 0.002	18.7 ± 0.001	< 0.0001	0.23
VEG	1.24 ± 0.007	1.24 ± 0.007	1.30 ± 0.005	< 0.0001	0.20

Continuation Table 2

COM	6.39 ± 0.003	6.39 ± 0.003	6.41 ± 0.002	< 0.0001	0.18
VARI	0.13 ± 0.002	0.12 ± 0.003	0.12 ± 0.002	= 0.0006	0.06

[1] Only the vegetation indices identified in the principal component analysis are shown. Leaves were considered deficient when showing a N content below 17 g N kg^{-1} DW; moderately deficient when showing a range from 17.1 to 20.0 g N kg^{-1} DW, and sufficient when showing a leaf N content above 20.1 g N kg^{-1} DW

Figure 1 - (A) Schematic diagram of the variations in chlorophyll a and b and carotenoids contents, the respective leaf spectral signature and the corresponding changes in the RGB color model of the images, representing plants with low N content (to the right) and high N content (to the left). Based on the responses shown in Hu *et al.* (2013), Rigon *et al.* (2016) and El-Azazy (2018). (B) Leaf samples and their variations in the RGB color model according to the different N status. Leaves were considered deficient when showing a N content below 17 g N kg^{-1} DW; moderately deficient when showing a range from 17.1 to 20.0 g N kg^{-1} DW, and sufficient when showing a leaf N content above 20.1 g N kg^{-1} DW

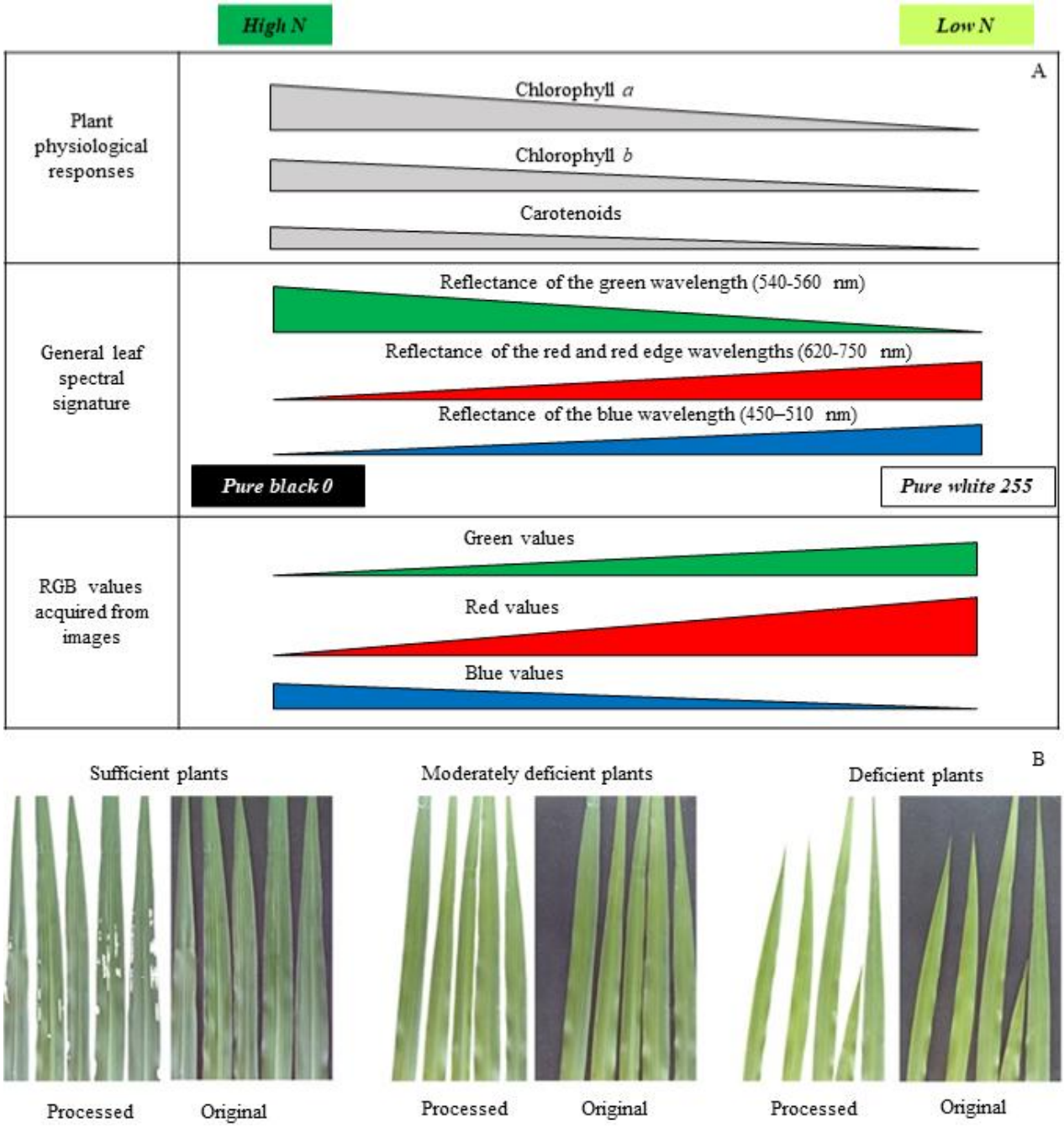

The same pattern of variation in the RGB components according to the leaf N gradients registered in this experiment was described for chlorophyll a, chlorophyll b and carotenoids by Rigon *et al.* (2016) in soybean (*Glycine max* L.) leaves, by Hu *et al.* (2013) in rice (*Oryza sativa* L.), and by Yadav, Ibaraki and Gupta (2010) in micropropagated potato (*Solanum tuberosum* L. cv. Benimaru) plants. The relationship between the individual RGB components and the leaf N followed a quadratic model, reaching the maximum value of red (139.4) at 24.4 g N kg^{-1} DW and green (162.4) at 25.0 g N kg^{-1} DW, whereas a minimum value of the blue component (120.8) was reached at 25.8 g N kg^{-1} DW. The quadratic relationships observed may explain the poor correlations registered among the individual RGB components and the leaf N, even with the wide range in the leaf N of the dataset (Table 2).

It is important to point out that, despite the general processes of light absorbance and reflectance for different wavelengths are well described in the literature, spectral signature is species-specific once it integrates plant physical (leaf thickness, serosity, leaf angle in the canopy) and physiological (e.g. pigments content) traits. It also interacts with environmental conditions, referred to in this paper as light conditions (wavelengths reflected or scattered by the surrounding vegetation, soil or clouds). Light conditions may remain 'printed' on the acquired images, particularly during sunrise/sunset, where a maximum of sun light spectrum shifts towards the red, which may change the color sensations and surface or crop color in digital imaging (ZILBERMAN *et al.*, 2018). Mata-Donjuan *et al.* (2012) highlighted that the RGB color space was not originally conceived for image processing but it was designed for computer graphics and, as a result, the RGB color space is very susceptible to light conditions during image acquisition procedures. According to Karcher and Richardson (2003), the intensity of red and blue can change the perception of greenness in a given image. In view of that, the HSB color space was used in a complementary way with the RGB color space in order to analyze possible effects of light conditions in the images acquired.

The exploratory analysis using the PCA identified that 88.6% of the dataset variance was explained by two principal components (Table 3), selecting 12 VIs (eigenvalues higher than 0.28). The first component explained 65% of the dataset variance and consisted of G_N, B_N, Saturation (S), ExG, CIVE, VEG and COM. The second component explained 23.6% of the dataset variance and it was comprising the R and G intensities of the images, Brightness (Br), ExR and VARIgreen. The normalized values of the blue channel (B_N) and the CIVE showed negative scores, whereas the normalized values

Table 3 - Eigenvalues, eigenvectors and scores of the vegetation indices (VIs) selected for the first two principal components (PRIN)

	PRIN1	PRIN2
Eigenvalues	11.70	4.25
Proportion	0.650	0.236
Accumulated	0.650	0.886
Criterion for cutting	0.28	0.28
[1]VIs	Eigenvectors	
R	0.045	0.440
G	0.130	0.319
G_N	0.289	-0.071
B_N	-0.284	-0.070
S	0.290	0.022
Br	0.130	0.319
ExG	0.289	-0.071
ExR	-0.120	0.391
CIVE	-0.288	0.080
VEG	0.284	-0.109
COM	0.282	-0.125
VARIgreen	0.086	-0.405

[1] R, G, G_N and B_N represent Red, Green, normalized Green and normalized Blue, respectively; S and Br represent saturation and brightness, respectively; ExG and ExR represent excess of green and excess of red, respectively; CIVE represents Colour Index of Vegetation Extraction; VEG represents the Vegetative Index; COM is a Combined Index and VARIgreen represents the Visible Atmospherically Resistant Index

of the green channel (G_N), the saturation values of the images (S) and the vegetation indices ExG, VEG and COM showed positive scores for the first component. For the second component, VARIgreen showed negative scores, while the pure values of red (R) and green channels (G), Brightness (Br) of the images and the excess of red (ExR) showed positive scores.

The PCA identified a positive correlation among G_N and saturation, but both were negatively associated with B_N. These relations can be observed by the increased B_N intensity associated with decreased G_N intensity and saturation as the leaf N increased. The observed saturation is related to the purity of the color, and less saturated images will appear closest to a gray color (near to zero). However, saturation not only depends upon the color of the subject or object but also upon the wavelengths of incident light, which make a given color in the image less saturated. Moreover, it is important to point out that in field images, under inconstant environmental light conditions, saturation is not uniform throughout the image. Karcher and Richardson (2003) showed that lower saturation levels appeared darker to the eye, and this was the case of images representing plants with sufficient N in the present experiment (Figure 1b). This pattern was also observed by Yadav, Ibaraki and Gupta (2010) when estimating the chlorophyll content in leaves of micro propagated potato (*Solanum tuberosum L.* cv. Benimaru) plants.

Brightness was also observed to be positively correlated with the red and green components, and with ExR in the images (Table 3), which was detected in the second component of the PCA. The brightness component is an indication of lightness or darkness of a color. Since it measures the proportion of brightness considering the maximum value between the RGB components compared to the maximum possible for the color (255), in our dataset this measurement reflects the intensity of the green component in the images. Similarly, Yang *et al.* (2015) showed that image spectral properties of brightness and saturation were negatively correlated with the chlorophyll content of micro propagated potato plants.

ANN topology and performance

With the selection of twelve VIs obtained by the PCA (Table 3), three types of neural networks were implemented. Yi *et al.* (2010) compared the prediction power of leaf N content in rice by using stepwise multiple linear regression (MLR) models and a neural network FFBP combined with two methods of selecting the input variables. Firstly, all spectral reflectance data were considered, but the maximum number of independent variables selected in the MLR model were set to five. In the second method, the scores of the first five principal components were used as independent variables. In both methods for selecting input variables, ANN modeling showed greater prediction power than MLR models, and the best performance was observed when using PCA to select the input variables ($R^2 = 0.94$ for calibration and $R^2 = 0.89$ for validation). A higher coefficient of determination and lower RMSE were also obtained using neural network compared to MLR models in Wang *et al.* (2009) for estimating the N concentration of oilseed rape (*Brassica napus* L.) from canopy reflectance data. According to the authors above, the reason for lower performance when using MLR is that the relationships between canopy reflectance and N concentration are nonlinear. Thus, the estimated N reaches a plateau and values would be underestimated at nitrogen concentrations greater than 2.5 when using MLR models. Zhang *et al.* (2012) observed that, compared to MLR models, ANNs had a strong advantage to fit the non-linear relationships between spectral signatures and the crude protein content in rice grain, reaching an $R^2 = 0.92$. The authors also highlighted that PCA was very useful as a method of data reduction, once some spectral parameters often contain redundant information.

The VIs selected by the PCA and the fertilization rate were inserted into the network as input data, while the N classes were adopted as the output of the network. Once the input and output parameters of the ANNs were defined, they were trained and tested by varying the type of network and the number of neurons in the hidden layer (Table 4). The best performance for the ANN tested were obtained with FFBP and CFBP both with the topology 13-5-1, and RBFNN with 13-148-1. It can be observed that the performance of FFBP compared to that of CFBP was slightly better with a maximum coefficient of determination (R^2) of 0.83 and accuracy of 88% compared to R^2 of 0.81 and accuracy of 86% for CFBP. When the RBFNN network was implemented, the performance reached $R^2 = 0.77$ and accuracy of 79%. Artificial neural networks have been widely used for estimating N status, chlorophyll and pigment contents in several species (MOHAN; GUPTA, 2019; SAFA *et al.*, 2019; ZHOU *et al.*, 2019; YI *et al.*, 2010), and also to classify and predict a variety of other parameters of vegetation (SHARABIANI; NAZARLOO; TAGHINEZHAD, 2019; ZHANG *et al.*, 2012). For this purpose, feedforward neural networks have been the most popular structures for modeling complex input-output relationships, in which the backpropagation learning algorithm is a well-known method.

One of the main differences thereof from the FFBP network is that in CFBP network there is a direct connection between input and output layers because each neuron in the input layer is attached to each neuron in the hidden layer. Besides, it is attached to each neuron in the

Table 4 - Summary table showing the performance of ANN model's topologies and internal parameters, where AF is the activation function, TF is the training function and LR is the learning rate

Network	Topology	AF	TF	LR	Performance				
					R^2 Train.	R^2 Valid	R^2 Test	R^2 General	[3]Accuracy (%)
FFBP	13-5-1	Tansig	[1]LM	0.1	0.85	0.81	0.79	0.83	88
CFBP	13-5-1	Tansig	LM	0.1	0.79	0.94	0.84	0.81	86
FFBP	13-10-1	Tansig	LM	0.1	0.78	0.82	0.77	0.79	80
CFBP	13-10-1	Tansig	LM	0.1	0.79	0.81	0.82	0.80	82
FFBP	13-15-1	Tansig	LM	0.1	0.77	0.76	0.86	0.79	80
CFBP	13-15-1	Tansig	LM	0.1	0.81	0.83	0.81	0.81	84
[2]RBFNN	13-148-1	Radial Base	[2]RBF	-	0.78	0.77	0.78	0.77	79

Input data (13) – R, G, G_N, B_N, S, Br, ExG, ExR, CIVE, VEG, COM, VARI and fertilization rates. [1] Levenberg-Marquardt (LM). [2] Radial basis function neural network with Radial Basis training function. The initialization of the initial center value determined from the input data was taken randomly, using the k-means algorithm; the Euclidean distance norm was defined to measure distance between input vector P and node j of the hidden layer, in which spread value was 1 and the goal 0.0001, and a Gaussian function transferred Euclidean distance to give output to each node. [3] Network accuracy in data prediction

output layer through a weight connection, meaning that each layer of neurons is related to all previous layers of neurons. Sharabiani, Nazarloo and Taghinezhad (2019) compared the performance for prediction of the protein content in winter wheat (*Triticum aestivum* L.) from canopy spectral reflectance using FFBP and CFBP neural networks. The performance was similar between them, but higher prediction power for both FFBP and CFBP was obtained when using the learning algorithm Levenberg-Marquardt (LM) compared to BFGS Quasi-Newton (BFG).

Vegetation traits have been accurately predicted using ANN models from the RGB in field images. Mohan and Gupta (2019) tested the performance of ANN models for prediction of leaf chlorophyll contents in rice from images acquired with a smartphone under natural light. The input data were based on several VIs calculated from the RGB and a combination of HSV and RGB color space models, and the authors above also observed improved efficiency of ANN models compared to MLR to predict leaf chlorophyll contents using RGB features. Similarly, Vesali *et al.* (2015) reported that ANNs were effective to estimate SPAD values accurately (RMSE = 5.1 and R^2 = 0.82) using image features extracted from the RGB and HSB color spaces as input data, even considering the fact that the measurements had been made under a range of different environmental conditions.

Although it has been well known that ANN modelling has a strong ability to learn, being effective to calibration, simulation and prediction of data, and is a convenient tool for depicting sophisticated non-linear systems and non-linear relationships that cannot be described by mathematical expressions (LI *et al.*, 2017), the use of radial basis function neural networks (RBFNN) is much less frequent for agricultural applications. The RBFNN is a typical three-layer feedforward network composed by an input layer, a nonlinear hidden layer, and a linear output layer (CHEN; COWAN; GRANT, 1991), which was built into a distance criterion with respect to a center. Two processing layers are required, in which, firstly, the input is mapped onto each radial basis function in the 'hidden' layer. The radial basis function defines a center and a radius, or a spread, to each neuron which is determined by training, and the performance of an RBFNN is widely affected by the chosen centers (CHEN; COWAN; GRANT, 1991). In the present experiment, a self-organized selection of centers using K-means clustering and Euclidean distance criterion was implemented. The second step is to estimate the connection weights, which were made using a Gaussian kernel function. Gautam and Panigrahi (2007) reported higher performance of RBFNN (R^2 = 0.82) compared to FFBP (R^2 = 0.76) for predicting leaf N content in corn plants under field conditions from spectral information in green and NIR bands. However, in the present experiment the accuracy (79%) obtained by using RBFNN was lower than any topology using FFBP and CFBP (Table 4).

The results showed that the proposed method can be used for software development aimed at monitoring N status in real time, providing a fast and inexpensive tool capable of defining the time of application and the amount of fertilizer in accordance with pasture demand.

Nitrogen fertilization management

For tropical pastures in Brazil, the traditional strategies for applying nitrogen fertilization are based on a fixed-rate split N at regular intervals (monthly) or applied after each grazing. Some intensive production systems have defined N fertilization rates based on an

Table 5 - Nitrogen content (mean – standard error, g N kg^{-1} leaf dry matter) of the sampled leaves according to the resulting classes of N status for each regrowth cycle, and the estimated fertilization rates (kg ha^{-1} of N per cutting) to attain sufficiency level for *Brachiaria brizhanta* 'Xaraes'

	Regrowth cycle			
Classes of N status[1]	Period 1 (December)	Period 2 (January)	Period 3 (February)	Period 4 (March)
(D) Deficient	15.0 ± 0.25	15.2 ± 0.34	15.8 ± 0.38	16.9 ± 0.48
Estimated N rate to attain sufficiency[2]	35	35	30	20
(MD) Moderately deficient	18.6 ± 0.38	18.2 ± 0.49	18.5 ± 0.27	18.6 ± 0.41
Estimated N rate to attain sufficiency	30	30	20	15
(S) Sufficient	19.8 ± 0.68	22.7 ± 0.27	22.8 ± 0.39	23.6 ± 0.27
Estimated N rate to attain sufficiency	0	0	0	0

[1] Leaves were considered deficient when showing a leaf N below 17 g N kg^{-1} DW; moderately deficient when showing a range from 17.1 to 20.0 g N kg^{-1} DW, and sufficient when showing a leaf N above 20.1 g N kg^{-1} DW. [2] Estimated N rate (ENR) calculated from equation $ENR=[(1/0.0081)*\ln(20/N_{content\ of\ the\ class})]$

empirical relation with the stocking rates expected, where 40 to 50 kg N ha^{-1} are applied for each animal unit (450 kg of animal live weight). According to Santos, Primavesi and Bernardi (2010), the total annual amount of N varies from 40 to 300 kg ha^{-1}, but there are no recommendations based on soil analysis or plant demand. The general relationship among N fertilization rates and leaf N content for the overall growth season was described by an exponential function ($N_{Leaf} = 15.61^{0.0081*NFertilizer}$, $R^2 = 0.60$), and it identified a requirement of approximately 30 to 35 kg ha^{-1} N after each cutting during the growth season. However, plants showed requirements for higher fertilization rates to reach the critical N content during the first regrowth, at the beginning of the growth season (Table 5). This period is characterized by an intense population renewal, when the major part of the tillers that survived the dry season die (CAMINHA *et al.*, 2010) and are replaced by young and highly productive tillers (PAIVA *et al.*, 2012). The above-ground growth is coordinated with a faster accumulation of root biomass, thus driving high N captures from the soil (KAMIJI *et al.*, 2014). At that regrowth cycle, plants that received less than 45 kg ha^{-1} of N after cutting were not able to reach an amount of N to fit in the sufficient class. In the following two regrowth cycles, lower fertilization rates were required, and the supply of 30 kg ha^{-1} N after cutting was enough to reach the sufficient class; whereas during the last regrowth cycle of the growth season only 15 kg ha^{-1} N after cutting could be recommended (Table 5).

Based on this approach and considering the experimental conditions of the site and the soil type, xaraes palisadegrass pastures would require a total amount of N fertilizer of approximately 120 kg ha^{-1} N during the growth season, but split at different rates, following the processes occurring at the plant population level. Shukla *et al.* (2004) pointed out that more than 60% of applied N can be lost when using fertilization at fixed-rates due to the lack of synchrony of plant N demand and N supply. For a rice (*Oryza sativa* L.) and wheat (*Triticum aestivum* L.) cropping system, the authors showed that fixed-time split N applications were not adequate for maintaining high yields and efficient use of N. On the other hand, when the time of application and the amount of fertilizer were carried out according to crop demand, the rice–wheat systems total productivity and farmer's profit were enhanced, resulting in net returns of 19 to 31% higher compared to that of fixed-time N applications. Bhatia *et al.* (2012) also reported environmental benefits of this approach for a rice–wheat system in India, with a reduction of nitrous oxide emissions by 16% and methane by 11% over the conventional split application of urea, concluding that tools for real-time N management represent a win–win option, thus reducing GHG emission and synchronizing N application with crop demand.

CONCLUSIONS

The ANNs showed good performance in the prediction of the N status (deficient, moderately deficient, or sufficient) of xaraes palisadegrass (*Brachiaria brizantha* 'Xaraes') pastures, indicating that image spectral signatures can be accurately determined from field images acquired with a cellphone camera. It was possible to reach a right classification rate (Accuracy) of 88% when using a FFBP artificial neural network, 86% when using a CFBP network and 79% when using a RBFNN network. All ANN models had a good power for classifying leaf images according their N status. However, the best performance was obtained with FFBP network.

ACKNOWLEDGEMENTS

The authors thank to São Paulo Research Foundation (FAPESP) by the support to this project (grant number 2020/00345-1), the Brazilian National Council for Scientific and Technological Development (CNPq) by the fellowship Productivity in Technological Development and Innovative Extension of Adriano R. B. Tech (314985/2018-2) and the Coordination for the Improvement of Higher Education Personnel (CAPES) for the support to perform this study.

REFERENCES

ATA-UL-KARIM, S. *et al.* Comparison of different critical nitrogen dilution curves for nitrogen diagnosis in rice. **Scientific Reports**, v. 7, n. 1, p. 1-14, 2017.

BARESEL, J. *et al.* Use of a digital camera as alternative method for non-destructive detection of the leaf chlorophyll content and the nitrogen nutrition status in wheat. **Computers and Electronics in Agriculture**, v. 140, p. 25-33, 2017.

BHATIA, A. *et al.* Greenhouse gas mitigation in rice–wheat system with leaf color chart-based urea application. **Environmental Monitoring and Assessment**, v. 184, n. 5, p. 3095-3107, 2012.

BURGOS-ARTIZZU, X. P. *et al*. Real-time image processing for crop/weed discrimination in maize fields. **Computers and Electronics in Agriculture**, v. 75, n. 2, p. 337-346, 2011.

CAMINHA, F. *et al*. Estabilidade da população de perfilhos de capim-marandu sob lotação contínua e adubação nitrogenada. **Pesquisa Agropecuária Brasileira**, v. 45, n. 2, p. 213-220, 2010.

CARDOSO, A. S. *et al.* Impact of the intensification of beef production in Brazil on greenhouse gas emissions and land use. **Agricultural Systems**, v. 143, p. 86-96, 2016.

CHEN, S.; COWAN, C. F. N.; GRANT, P. M. Orthogonal least squares learning algorithm for radial basis function networks. **IEEE Transactions on Neural Networks**, v. 2, n. 2, p. 302- 309, 1991.

COSTA, J. P. R. *et al.* Relative chlorophyll contents in the evaluation of the nutritional status of nitrogen from xaraes palisade grass and determination of critical nitrogen sufficiency index. **Acta Scientiarum**. **Animal Sciences**, v. 37, n. 2, p. 109-114, 2015.

EL-AZAZY, A. M. Inspect the potential of using leaf image analysis procedure in estimating nitrogen status in citrus leaves. **Middle East Journal of Agriculture Research**, v. 7, n. 3, p. 1059-1071, 2018.

EMPRESA BRASILEIRA DE PESQUISA AGROPECUÁRIA. **Banco de dados climáticos do Brasil**. 2019. Disponível em: https://www.cnpm.embrapa.br/projetos/bdclima. Acesso em: 28 ago. 2019.

EMPRESA BRASILEIRA DE PESQUISA AGROPECUÁRIA. **Sistema brasileiro de classificação de solos**. Rio de Janeiro, 2018. 356 p.

GAUTAM, R.; PANIGRAHI, S. Leaf nitrogen determination of corn plant using aerial images and artificial neural networks. **Canadian Biosystems Engineering**, v. 49, n. 7, p. 1-7, 2007.

GITELSON, A. A. *et al*. Novel algorithms for remote estimation of vegetation fraction. **Remote Sensing of Environment**, v. 80, n. 1, p. 76-87, 2002.

GUIJARRO, M. *et al*. Automatic segmentation of relevant textures in agricultural images. **Computers and Electronics in Agriculture**, v. 75, n. 1, p. 75-83, 2011.

HE, B. *et al.* Estimating monthly total nitrogen concentration in streams by using artificial neural network. **Journal of Environmental Management**, v. 92, n. 1, p. 172-177, 2011.

HU, H. *et al.* Estimation of leaf chlorophyll content of rice using image color analysis. **Canadian Journal of Remote Sensing**, v. 39, n. 2, p. 185-190, 2013.

INTARAVANNE, Y.; SUMRIDDETCHKAJORN, S. Android-based rice leaf color analyzer for estimating the needed amount of nitrogen fertilizer. **Computers and Electronics in Agriculture**, v. 116, p. 228-233, 2015.

KAMIJI, Y. *et al.* Shoot biomass in wheat is the driver for nitrogen uptake under low nitrogen supply, but not under high nitrogen supply. **Field Crops Research**, v. 165, p. 92-98, 2014.

KARCHER, D. E.; RICHARDSON, M. D. Quantifying turfgrass color using digital image analysis. **Crop Science**, v. 43, n. 3, p. 943-951, 2003.

LEE, K.; LEE, B. Estimation of rice growth and nitrogen nutrition status using color digital camera image analysis. **European Journal of Agronomy**, v. 48, p. 57-65, 2013.

LI, Y. *et al*. Machine learning for the prediction of *L. chinensis* carbon, nitrogen and phosphorus contents and understanding of mechanisms underlying grassland degradation. **Journal of Environmental Management**, v. 192, p. 116-123, 2017.

MATA-DONJUAN, G. F. *et al.* Use of improved hue, luminance and saturation (IHLS) color space in the estimation of nitrogen on tomato seedlings (*Lycopersicon esculentum*). **Scientific Research and Essays**, v. 7, n. 27, p. 2343-2349, 2012.

MAZZETTO, A. M. *et al.* Improved pasture and herd management to reduce greenhouse gas emissions from a Brazilian beef production system. **Livestock Science**, v. 175, p. 101-112, 2015.

MOHAN, P. J.; GUPTA, S. D. Intelligent image analysis for retrieval of leaf chlorophyll content of rice from digital images of smartphone under natural light. **Photosynthetica**, v. 57, n. 2, p. 388-398, 2019.

NOGUEIRA, A. D. A. *et al.* **Manual de laboratório**: solo, água, nutrição vegetal, nutrição animal e alimentos. São Carlos: Embrapa-CPPSE, 1998.

PAIVA, A. *et al*. Structural characteristics of tiller age categories of continuously stocked marandu palisade grass swards fertilized with nitrogen. **Revista Brasileira de Zootecnia**, v. 41, n. 1, p. 24-29, 2012.

PEDREIRA, B. C.; PEDREIRA, C. G.; SILVA, S. C. Estrutura do dossel e acumulo de forragem de *Brachiaria brizantha*

cultivar xaraes em resposta a estratégias de pastejo. **Pesquisa Agropecuária Brasileira**, v. 42, n. 2, p. 281-287, 2007.

RAHMAT, R.; NABABAN, E. Classification of rice plant fertilizer needs based on leaf color chart using radial basis function neural network. **Journal of Physics: Conference Series**, v. 1116, n. 2, p. 022037, 2018.

RIGON, J. P. G. *et al*. A novel method for the estimation of soybean chlorophyll content using a smartphone and image analysis. **Photosynthetica**, v. 54, n. 4, p. 559-566, 2016.

SAFA, M. *et al*. Modelling nitrogen content of pasture herbage using thermal images and artificial neural networks. **Thermal Science and Engineering Progress**, v. 11, p. 283-288, 2019.

SANTOS, P.; PRIMAVESI, O.; BERNARDI, A. Adubação de pastagens. *In*: PIRES, A. V. (ed.). **Bovinocultura de corte**. Piracicaba: FEALQ, 2010. p. 459-471.

SCHLICHTING, A. *et al*. Efficiency of portable chlorophyll meters in assessing the nutritional status of wheat plants. **Revista Brasileira de Engenharia Agrícola e Ambiental**, v. 19, n. 12, p. 1148-1151, 2015.

SHARABIANI, V.; NAZARLOO, A. S.; TAGHINEZHAD, E. Prediction of protein content of winter wheat by canopy of near infrared spectroscopy (NIRS), using partial least squares regression (PLSR) and artificial neural network (ANN) models. **Yüzüncü Yıl Üniversitesi Tarım Bilimleri Dergisi**, v. 29, n. 1, p. 43-51, 2019.

SHUKLA, A. *et al.* Calibrating the leaf color chart for nitrogen management in different genotypes of rice and wheat in a systems perspective. **Agronomy Journal**, v. 96, n. 6, p. 1606-1621, 2004.

SILVA, R. de O. *et al.* Sustainable intensification of Brazilian livestock production through optimized pasture restoration. **Agricultural Systems**, v. 153, p. 201-211, 2017.

SRIDEVY, S. *et al.* Nitrogen and potassium deficiency identification in maize by image mining, spectral and true colour response. **Indian Journal of Plant Physiology**, v. 23, n. 1, p. 91-99, 2018.

TEWARI, V. *et al.* Estimation of plant nitrogen content using digital image processing. **Agricultural Engineering International: CIGR Journal**, v. 15, n. 2, p. 78-86, 2013.

VERGARA-DÍAZ, O. *et al*. A novel remote sensing approach for pre-diction of maize yield under different conditions of nitrogen fertilization. **Frontiers in Plant Science**, v. 7, p. 666, 2016.

VESALI, F. *et al*. Development of an android app to estimate chlorophyll content of corn leaves based on contact imaging. **Computers and Electronics in Agriculture**, v. 116, p. 211-220, 2015.

WANG, Y. *et al.* Estimating rice chlorophyll content and leaf nitrogen concentration with a digital still color camera under natural light. **Plant Methods**, v. 10, n. 1, p. 36, 2014.

WANG, Y. *et al*. Validation of artificial neural network techniques in the estimation of nitrogen concentration in rape using canopy hyperspectral reflectance data. **International Journal of Remote Sensing**, v. 30, n. 17, p. 4493- 4505, 2009.

YADAV, S.; IBARAKI, Y.; GUPTA, S. Estimation of the chlorophyll content of micropropagated potato plants using RGB based image analysis. **Plant Cell, Tissue and Organ Culture (PCTOC)**, v. 100, n. 2, p. 183-188, 2010.

YANG, W. *et al*. Greenness identification based on HSV decision tree. **Information Processing in Agriculture**, v. 2, n. 3/4, p. 149-160, 2015.

YASUOKA, J. I. *et al.* Canopy height and n affect herbage accumulation and the relative contribution of leaf categories to photosynthesis of grazed *Brachiaria* grass pastures. **Grass and Forage Science**, v. 73, n. 1, p. 183-192, 2018.

YI, Q. *et al.* Evaluating the performance of PC-ANN for the estimation of rice nitrogen concentration from canopy hyperspectral reflectance. **International Journal of Remote Sensing**, v. 31, n. 4, p. 931-940, 2010.

YI, Q. X. *et al*. Monitoring rice nitrogen status using hyperspectral reflectance and artificial neural network. **Environmental Science & Technology**, v. 41, n. 19, p. 6770-6775, 2007.

ZHANG, H. *et al*. Prediction of crude protein content in rice grain with canopy spectral reflectance. **Plant, Soil and Environment**, v. 58, n. 11, p. 514-520, 2012.

ZHOU, C. *et al.* Imaging analysis of chlorophyll fluorescence induction for monitoring plant water and nitrogen treatments. **Measurement**, v. 136, p. 478-486, 2019.

ZHU, Y.; HUANG, C. An improved median filtering algorithm for image noise reduction. **Physics Procedia**, v. 25, p. 609-616, 2012.

ZILBERMAN, A. *et al.* Applicability of digital color imaging for monitoring nitrogen uptake and fertilizer requirements in crops. *In*: **Remote Sensing for Agriculture, Ecosystems, and Hydrology XX**. International Society for Optics and Photonics, 2018. p. 107831Y.